

PAPER

View Article Online
View Journal | View Issue

Cite this: RSC Adv., 2019, 9, 6770

tert-Butylphenylthiazoles with an oxadiazole linker: a novel orally bioavailable class of antibiotics exhibiting antibiofilm activity†

Ahmed Kotb,^{†a} Nader S. Abutaleb,^{†b} Mohamed Hagra,^a Ashraf Bayoumi,^a Mahmoud M. Moustafa,^c Adel Ghiaty,^a Mohamed N. Seleem^{*bd} and Abdelrahman S. Mayhoub^{ib*ae}

The structure–activity and structure–kinetic relationships of a new *tert*-butylphenylthiazole series with oxadiazole linkers were conducted with the objective of obtaining a new orally available antibacterial compounds. Twenty-two new compounds were prepared, purified and identified. Their activity against methicillin-resistant *Staphylococcus aureus* were examined. Compound **20** with 3-hydroxyazetidine as a nitrogenous side chain showed promising activity against twenty-four clinical isolates, including vancomycin-resistant staphylococcal and enterococcal species with MIC values ranging from 4–8 $\mu\text{g mL}^{-1}$. Additional advantages of this compound include an ability to eradicate staphylococcal biofilm mass in a dose-dependent manner as well as high metabolic stability after an oral dose of 25 mg kg^{-1} with a biological half-life that exceeds 5 hours and a plasma concentration (C_{max}) that exceeds the MIC values.

Received 23rd December 2018

Accepted 16th February 2019

DOI: 10.1039/c8ra10525a

rsc.li/rsc-advances

1. Introduction

The rapid development of antimicrobial resistance is a major global health concern due to the exponentially decreased utility of antibiotics available for clinicians. The World Health Organization (WHO) recently reported a set of innovation criteria for new antibiotic developments in order to maintain long-term clinical efficacy.¹ These criteria include introducing novel chemical scaffolds, broad spectrum activity *versus* multidrug-resistant strains, and targeting novel pathways.¹ These criteria are met by our newly-developed arylthiazole **1a**, as an inhibitor of two novel proteins (undecaprenyl pyrophosphatase and undecaprenyl pyrophosphate synthase) involved in the peptidoglycan synthesis.^{2–5} However, the main drawback of **1a** (Fig. 1) was the extremely short plasma half-life, for which the $t_{1/2}$ was only 29 minutes.⁵ The benzylic

methylene carbon was identified as a metabolic soft spot.⁶ The replacement of the *n*-alkyl moiety with branched *tert*-butyl or alkoxy analogues provided more metabolically-stable derivatives with enhanced antibiofilm activity.^{6,7} We did additional structural modification focused on the C=N linker, where it has been replaced with different heterocyclic rings.¹ Of the tested heterocyclic linkers,^{4,5,8} only the oxadiazole-containing derivatives were orally bioavailable.¹

In this study, we address the structure–activity and structure–kinetic relationships of the oxadiazole based hybrid scaffold **1b** at position-5 (Fig. 1), aiming to prepare new derivatives with enhanced antibacterial activity against multidrug-resistant staphylococcal strains, improved oral bioavailability and antibiofilm activity.

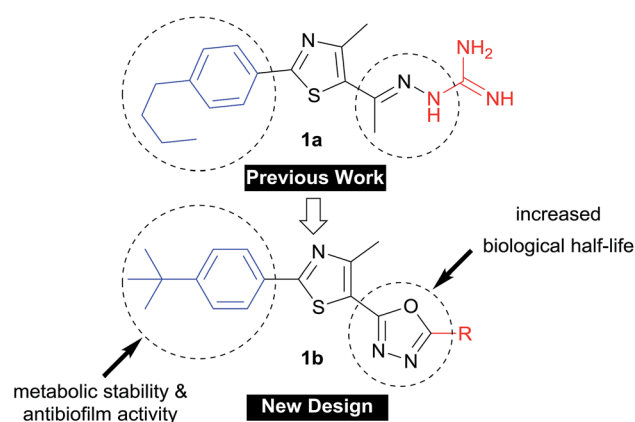


Fig. 1 Progress in the development of phenylthiazole antibiotics.

^aDepartment of Pharmaceutical Organic Chemistry, College of Pharmacy, Al-Azhar University, Cairo 11884, Egypt. E-mail: amayhoub@azhar.edu.eg

^bDepartment of Comparative Pathobiology, College of Veterinary Medicine, Purdue University, West Lafayette, IN, USA 47907. E-mail: mseleem@purdue.edu

^cDepartment of Pharmaceutical Chemistry, Imam Abdulrahman Bin Faisal University, Dammam 31441, Saudi Arabia

^dPurdue Institute of Inflammation, Immunology, and Infectious Disease, West Lafayette, IN, USA, 47907

^eUniversity of Science and Technology, Nanoscience Program, Zewail City of Science and Technology, October Gardens, 6th of October, Giza 12578, Egypt

† Electronic supplementary information (ESI) available: Scanned copies of all spectral data of all new reported compounds. See DOI: 10.1039/c8ra10525a

‡ These two authors contributed equally.

2. Results and discussion

2.1. Chemistry

The synthesis of the target compounds started with the preparation of phenylthiazole ethyl ester **3** from commercially available thioamide **2**. The treatment of ethyl ester **3** with hydrazine hydrate provided the corresponding acid hydrazide **4**, which was converted into methylmercapto-1,3,4-oxadiazole upon reaction with carbon disulfide followed by the methylation of the free mercaptyl group with dimethyl sulphate (Scheme 1). The oxidation of the methylmercaptyl moiety with chloroperbenzoic acid furnished the key intermediate **7**, which was then utilized to prepare the entire series of oxadiazolylphenylthiazole final products **8–30**.

The chemical structures of the newly synthesized compounds were confirmed *via* spectral and elemental data. For instance, the ethoxy group of compound **3** was represented in the ^1H NMR spectrum by two signals at 4.33 and 1.13 ppm. These two distinguished signals were replaced with two broad singlets at δ 9.57 and 4.54 when treated with hydrazine hydrate (compound **4**). Upon cyclization with carbon disulfide and

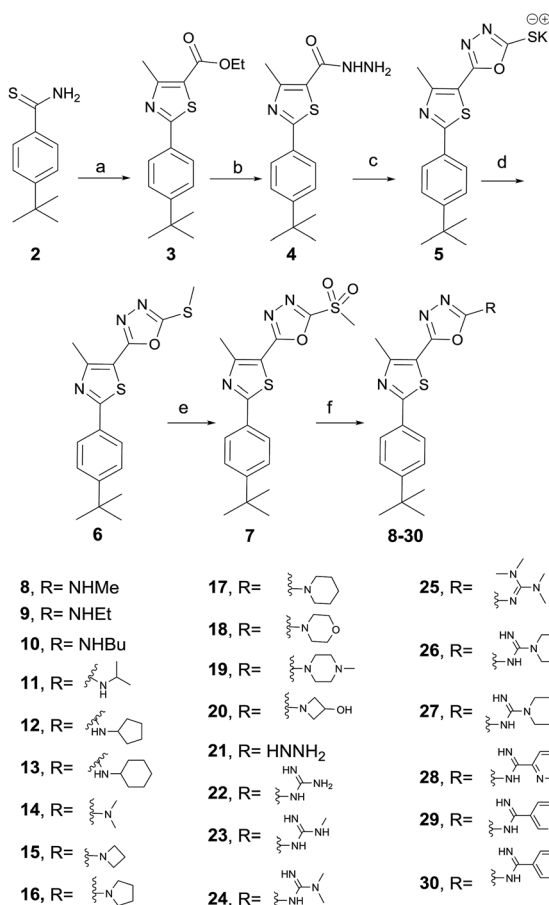
methylation with dimethylsulfate, the broad signals disappeared and an additional singlet signal in the aliphatic region, appeared at δ 2.77, a characteristic of *S*-methyl (compound **5**). Upon oxidation with *m*CPBA (compound **6**), this particular signal shifted downfield to 3.47 ppm, and disappeared following the treatment of **6** with nitrogenous based nucleophiles. Among compounds **7–12**, the characteristic methylsulfonyl moieties signal at 3.47 ppm disappeared from the ^1H NMR spectra and was replaced with a broad singlet at approximately 7.83 ppm due to the NH group as well as the presence of extra aliphatic protons equivalent to the number of aliphatic side chains connected with the terminal amine. Collectively, these findings confirm the tethering of the nucleophile moiety with the oxadiazole position-5. For example, the ^1H NMR spectrum of compound **10** showed, in addition to the oxadiazolylphenylthiazole nucleus protons, a broad singlet signal equivalent to one proton at δ 7.82 due to NH in addition to a multiplet signal equivalent to one proton and a doublet signal for six protons at δ 3.70 and 1.20, respectively, due to an isopropyl side chain. For the tertiary-amine side-chain-containing compounds **13–19**, the most predominant features of the ^1H NMR isolated products spectra were the disappearance of the methylsulfonyl singlet at 3.47 ppm and the appearance of a set of distinctive signals in the upper field region due to the corresponding protons of the alkyl nucleophile moieties. On the other hand, the hydrazinyl group of compound **20** was represented in the ^1H NMR by two broad singlets at 6.94 and 4.54 ppm, due to NH and NH_2 moieties, respectively.

Additionally, the ^1H NMR spectrum of the guanidine-containing derivative **21** displayed two broad singlets at 7.21 and 7.06 ppm due to guanidine protons, as well as signals corresponding to the oxadiazolylphenylthiazole nucleus. The ^1H NMR spectra of the carboximide-containing nucleophiles, compounds **24–28**, showed two broad singlets peaks due to NH and $\text{C}=\text{NH}$ protons, in addition to the disappearance of the methylsulfonyl singlet peak at 3.47 ppm.

2.2. Biological results and discussion

2.2.1. Antibacterial activity. At the outset of this study, the initial antibacterial screening was performed on methicillin-resistant *Staphylococcus aureus* (MRSA, 2658 RCMB). The results presented in Table 1 indicated that the 2-amino-1,3,4-oxadiazole linker with aliphatic side chains (compounds **8–17**) is void of anti-MRSA activity.

In contrast, the more polar side chains—morpholine, piperazine and hydroxyazetidine—provided the desired antibacterial activity, the maximum potency obtained from hydroxyazetidine-containing derivative **20**, and inhibited the growth of MRSA at a minimum-inhibitory-concentration (MIC) of $3.1\ \mu\text{g mL}^{-1}$ (one fold higher than the MIC of vancomycin against the same strain) (Table 1). Further expansion of the nitrogenous side chain provided the hydrazinyl and guanidinyll derivatives **21** and **22**, both of which had a one-fold less potency than the parent compound **20**. Derivatives with additional cyclic nitrogenous moieties (compounds **26–30**) were found to be inactive or less active than the lead compound **20** (Table 1).



Scheme 1 Synthesis of compounds **8–30**. Reagents and conditions: (a) ethyl 2-chloro-3-oxobutanoate, absolute EtOH, heat at reflux, 4 h; (b) absolute EtOH, $\text{NH}_2\text{NH}_2 \cdot \text{H}_2\text{O}$, heat at reflux, 8 h; (c) CS_2 , KOH, EtOH, heat reflux, 12 h; (d) dimethyl sulfate, H_2O , stirring at 23°C , 2 h; (e) *m*CPBA, dry DCM, 23°C , 16 h; (f) appropriate amine, hydrazine, guanidine or carboximide; K_2CO_3 , DMF, heat at 80°C for 0.5–12 h.

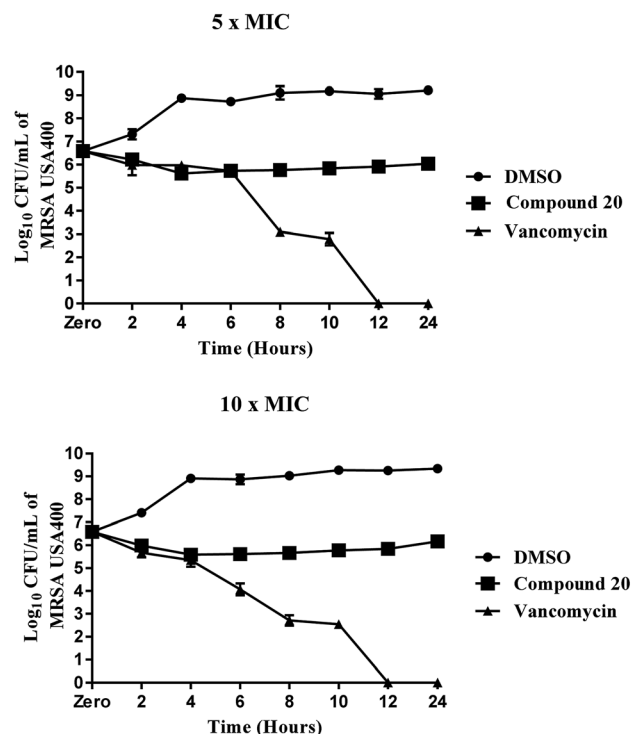


Table 1 Initial MIC screening of the compounds against methicillin-resistant *Staphylococcus aureus* (2658 RCMB)

Compound	MRSA (2658 RCMB)	Compound	MRSA (2658 RCMB)
8	50	20	3.12
9	>50	21	6.25
10	>50	22	6.25
11	>50	23	12.5
12	>50	24	12.5
13	>50	25	25
14	>50	26	25
15	>50	27	25
16	>50	28	>50
17	>50	29	>50
18	6.25	30	>50
19	6.25	Vancomycin	1.56

To further assess the antibacterial potency of this new class of arylthiazoles, the most promising derivative **20** was selected and its anti-staphylococcal activity was tested against twenty-four clinical isolates (Table 2).

Compound **20** exhibited moderate antibacterial activity against all methicillin-sensitive *S. aureus* (MSSA) and tested MRSA strains at concentrations ranging from 4 to 16 $\mu\text{g mL}^{-1}$. Its MBC values were higher than 64 $\mu\text{g mL}^{-1}$, more than threefold higher than its MIC values against the tested strains and evidence that the compound is a bacteriostatic agent. This mode of anti-staphylococcal inhibition was further confirmed using a time-killing assay at two different concentrations (5×

**Fig. 2** Time-kill assay of compound **20** and vancomycin tested in triplicates (at 5× MIC and 10× MIC) against methicillin-resistant *Staphylococcus aureus* (MRSA USA400) over a 24 hour incubation period at 37 °C. DMSO (solvent for the compound) served as a negative control. The error bars represent standard deviation values.**Table 2** The minimum inhibitory concentration (MIC in $\mu\text{g mL}^{-1}$) and minimum bactericidal concentration (MBC in $\mu\text{g mL}^{-1}$) of compound **20** against a panel of *Staphylococcus aureus* clinically relevant strains

Bacterial strains	Compound 20		Vancomycin	
	MIC	MBC	MIC	MBC
MSSA ATCC 6538	4	>64	1	2
MSSA NRS 107	4	>64	2	2
MRSA NRS 108	4	>64	1	2
MRSA NRS 194	8	>64	1	1
MRSA NRS 119	8	>64	1	1
MRSA NRS 382 (USA 100)	16	>64	2	2
MRSA NRS 383 (USA 200)	8	>64	1	1
MRSA NRS384 (USA 300)	4	>64	1	1
MRSA NRS123 (USA 400)	8	>64	1	1
MRSA NRS 385 (USA 500)	4	>64	0.5	1
MRSA NRS 386 (USA 700)	8	>64	1	1
MRSA NRS 387 (USA 800)	4	>64	0.5	0.5
MRSA NRS 483 (USA 1000)	8	>64	1	1
MRSA NRS 484 (USA 1100)	8	>64	2	2
VISA NRS 1	4	>64	4	4
VISA NRS 19	8	>64	4	4
VISA NRS 37	4	>64	4	8
VRSA 2	4	>64	64	64
VRSA 5	8	>64	>64	>64
VRSA 6	8	>64	>64	>64
VRSA 7	8	>64	>64	>64
VRSA 9	8	>64	>64	>64
VRSA 10	8	>64	64	>64
VRSA 11a	8	>64	>64	>64

MIC and 10× MIC) (Fig. 2). Despite a moderate potency against MRSA clinical isolates, compound **20** maintained its antibacterial potency against all nine-tested vancomycin-intermediate and vancomycin-resistant *Staphylococcus aureus* strains (VISA and VRSA). These findings suggest the advantages of this compound over vancomycin, the drug of choice for the treatment of invasive staphylococcal infections.

Similar to the results obtained with *S. aureus* strains, compound **20** exhibited moderate antibacterial activity against other clinically-important Gram-positive pathogens, and inhibited the growth of the tested strains at concentrations of 4 to 16 $\mu\text{g mL}^{-1}$ (Table 3).

Most importantly, compound **20** also maintained its potency against vancomycin-resistant enterococci strains (*i.e.* vancomycin-resistant *Enterococcus faecium* and *Enterococcus faecalis*) (Table 3). Vancomycin-resistant enterococci (VRE) are a leading cause of healthcare-associated infections. VRE colonization can eventually lead to life-threatening endocarditis and urinary tract infections.^{9–11} *E. faecium* is of high clinical interest and responsible for the vast majority of nosocomial enterococcal infections that result in patients with vancomycin-resistant enterococcal endocarditis with limited therapeutic options. Moreover, the MBC values for compound **20** against the tested strains were more than threefold higher than its MIC values, evidence that compound **20** may be bacteriostatic against these strains. In addition, the preliminary safety profile of compound **20** was evaluated against two types of cell (vero



Table 3 The minimum inhibitory concentration (MIC in $\mu\text{g mL}^{-1}$) and minimum bactericidal concentration (MBC in $\mu\text{g mL}^{-1}$) of compound **20** against a panel of Gram-positive bacterial pathogens

Bacterial strains	Compound 20		Vancomycin	
	MIC	MBC	MIC	MBC
Methicillin-resistant <i>S. epidermidis</i> NRS101	4	>64	1	1
<i>Enterococcus faecalis</i> ATCC 51299 (VRE)1	16	>64	32	64
<i>Enterococcus faecium</i> ATCC 700221 (VRE)1	8	>64	>64	>64
<i>Listeria monocytogenes</i> ATCC 19111	8	>64	1	1
Cephalosporin-resistant <i>Streptococcus pneumoniae</i> ATCC 51916	16	>64	1	1
Methicillin-resistant <i>Streptococcus pneumoniae</i> ATCC 700677	16	>64	2	4

and caco-2 cells) and it showed high tolerability against both (Fig. 1S and 2S†).

2.2.2. Antibiofilm activity. Given that approximately 65% of current human microbial infections are biofilms,¹² it is predicted that biofilm will be the major source of future bacterial infections. Biofilm is a surmountable barrier to most of the antibiotic arsenal. Hence, common antibiotics such as penicillin and ciprofloxacin are losing their potency as a result of biofilm-induced infections.¹³ Staphylococci (in particular *S. aureus* and *S. epidermidis*) cause various biofilm-related infections.¹⁴ They tend to form harmful biofilms on implanted prosthetic devices and tissues.¹⁵ Few antibacterial agents can disrupt these biofilms (MRSA biofilms in particular). Therefore, we evaluated the capacity of compound **20** to disrupt mature MRSA biofilm. Due to its large molecular structure and polar nature, vancomycin is unable to effectively penetrate such bacterial biofilms. At $1 \times \text{MIC}$, vancomycin disrupted only about 8% of the MRSA biofilm (Fig. 3). This value increased to around 18% eradication of adherent biofilm when the concentration was doubled. Even at a concentration of $32 \times \text{MIC}$, vancomycin was only capable of reducing the biofilm mass by 34% (data not published). Remarkably, the hydroxyzetidine derivative **20** was superior to vancomycin in MRSA biofilm eradication and

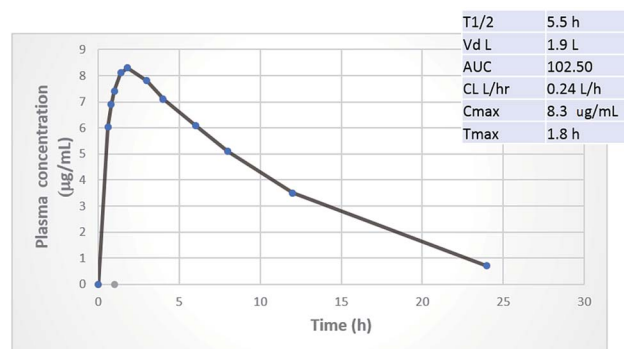


Fig. 4 Oral pharmacokinetic curve and key PK parameters in the rat after 25 mg kg^{-1} oral dose of compound **20**.

exhibited a concentration-dependent biofilm disruption (Fig. 3). At $1 \times \text{MIC}$, compound **20** disrupted 13% of the mature MRSA300 biofilm mass. This increased to about 41% eradication of the adherent biofilm when its concentration was increased by one-fold ($2 \times \text{MIC}$) (Fig. 3).

2.2.3. In vivo pharmacokinetic evaluation. The principal challenge of designing an orally administered antibiotic is that its plasma concentration has to exceed its MIC values. So far, most of the newly-introduced antibiotics, such as ceftaroline¹⁶ and lipoglycopeptides are taken parenterally.¹⁷ When phenylthiazoles were first discovered, their main drawback was the extremely short plasma half-life of the early generation, for which the $t_{1/2}$ of the lead compound **1** (Fig. 1) was only 29 minutes.² To assess whether the chemical modifications presented in this study have the expected positive impact on the pharmacokinetic profile, a rat was administered a 25 mg kg^{-1} oral dosage of compound **20**. Fig. 4 indicates that compound **20** possesses high metabolic stability with a biological half-life of 5.5 hours and low clearance rate. Most importantly, compound **20** reaches a plasma concentration that surpasses its MIC values against most of the tested multidrug-resistant clinical isolates.

3. Conclusions

Building a hybrid scaffold with the *t*-butylphenyl lipophilic part and oxadiazole linker followed by a study of the proper

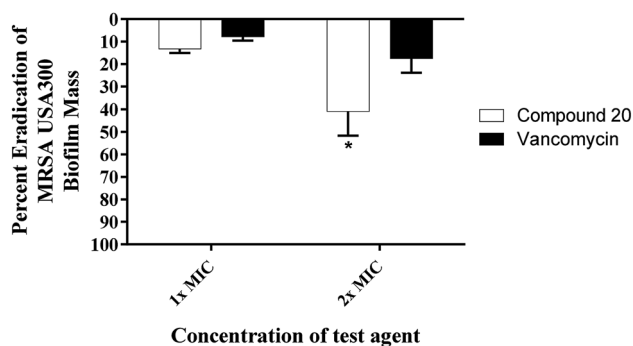


Fig. 3 Efficiency of compound **20** and vancomycin (tested in quartets) in disrupting the established MRSA biofilm. Data are presented as percent eradication of MRSA USA300 mature biofilm compared to the control (DMSO; the solvent for the tested compound). Error bars represent standard deviation values. Asterisk (*) denotes statistical significance ($P < 0.05$) between results for compound **20** and vancomycin analyzed via one-way ANOVA with *post hoc* Dennett's test for multiple comparisons.



nitrogenous substituent at oxadiazole position-5 provided compound **20** with 3-hydroxyazetidine moiety as the most promising derivative. Interestingly, the unsubstituted azetidinyll analogue **15** was void of any antibacterial activity. The moderate antibacterial potency of hydroxyazetidinyll derivative **20**, when tested against around thirty Gram-positive multidrug-resistant strains, was advantageous over vancomycin, the drug of choice for the treatment of invasive, life-threatening staphylococcal infections, and effective against all tested vancomycin-resistant species (*i.e.* VRSA and VRE). Furthermore, it was highly tolerable on vero cells and caco-2 cells. Moreover, compound **20** was more than two-fold better than vancomycin in its ability to disrupt bacterial biofilm mass. Another advantage of compound **20** over vancomycin and other phenylthiazoles is its highly acceptable pharmacokinetic profile: a biological half-life that is 11-fold more than the lead compound **1a** with oral absorbability.

4. Experimental

4.1. General

¹H NMR spectra were run at 400 MHz and ¹³C NMR spectra were determined at 100 MHz in deuterated chloroform (CDCl₃), or dimethyl sulfoxide (DMSO-*d*₆) on a Varian Mercury VX-400 NMR spectrometer. Chemical shifts are given in parts per million (ppm) on the delta (δ) scale. Chemical shifts were calibrated relative to those of the solvents. Flash chromatography was performed on 230–400 mesh silica. The progress of reactions was monitored with Merck silica gel IB2-F plates (0.25 mm thickness). The infrared spectra were recorded in potassium bromide disks on pye Unicam SP 3300 and Shimadzu FT IR 8101 PC infrared spectrophotometer. Mass spectra were recorded at 70 eV. High-resolution mass spectra for all ionization techniques were obtained from a FinniganMAT XL95. Melting points were determined using capillary tubes with a Stuart SMP30 apparatus and are uncorrected. All yields reported referring to isolated yields.

4.1.1. Ethyl 2-(4-(*tert*-Butyl)phenyl)-4-methylthiazole-5-carboxylate (3). Compound **2** (3 g, 14 mmol) and ethyl 2-chloro-3-oxobutanoate (3.88 mL, 4.62 g, 28 mmol) were added to absolute ethanol (30 mL). The reaction mixture was heated at reflux for 4 h. After removal of solvent under reduced pressure, the solid residue was purified by crystallization from ethanol to provide the desired product as white crystals (4.4 g, 95%) mp = 105 °C; ¹H NMR (DMSO-*d*₆) δ: 7.79 (d, *J* = 8.4 Hz, 2H), 7.49 (d, *J* = 8.4 Hz, 2H), 4.33 (q, *J* = 4.8 Hz, 2H), 2.67 (s, 3H), 1.29 (s, 9H), 1.13 (t, *J* = 4.8 Hz, 3H); ¹³C NMR (DMSO-*d*₆) δ: 169.1, 154.5, 153.8, 139.5, 130.8, 126.7, 126.1, 115.3, 61.8, 35.1, 28.8, 17.7, 14.5; MS (*m/z*) 303; anal. calc. for: (C₁₇H₂₁NO₂S): C, 67.30; H, 6.98; N, 4.62%; found: C, 67.32; H, 6.99; N, 4.63%.

4.1.2. 2-(4-(*tert*-Butyl)phenyl)-4-methylthiazole-5-carbohydrazide (4). To a solution of **3** (1.29 g, 4 mmol) in ethanol (15 mL), hydrazine hydrate (99%, 1 mL, 20 mmol) was added dropwise. The reaction mixture was heated at reflux for 8 h then allowed to cool down to room temperature. The formed solid was separated by filtration and crystallized from ethanol to provide the desired product as white crystals (1.1 g, 93%) mp = 204–205 °C; ¹H NMR (DMSO-*d*₆) δ: 9.57 (brs, 1H), 7.82 (d, *J* =

8.4 Hz, 2H), 7.49 (d, *J* = 8.4 Hz, 2H), 4.54 (brs, 2H), 2.65 (s, 3H), 1.30SS (s, 9H); ¹³C NMR (DMSO-*d*₆) δ: 165.6, 155.2, 153.5, 142.3, 130.9, 126.7, 126.4, 115.3, 35.1, 18.7, 17.3; MS (*m/z*) 289; anal. calc. for: (C₁₅H₁₉N₃OS): C, 62.26; H, 6.62; N, 14.52%; found: C, 62.27; H, 6.63; N, 14.53%.

4.1.3. 2-(2-(4-(*tert*-Butyl)phenyl)-4-methylthiazol-5-yl)-5-(methylthio)-1,3,4-oxadiazole (6). Potassium hydroxide (0.4 g, 10 mmol) was added to a solution of **4** (3 g, 10 mmol) in ethanol (15 mL), followed by drop-wise addition of carbon disulphide (3 mL, 110 mmol) over 0.5 h. The reaction mixture was stirred at room temperature for an additional 15 min and then heated to reflux until the evolution of hydrogen sulfide gas ceased. After completion of the reaction, as monitored by TLC, the obtained intermediate was poured on cold water (50 mL), filtered, washed with water, dried and crystallized from ethanol to provide potassium salt **5** as yellow crystals (3.4 g, 89%) mp > 300 °C; ¹H NMR (DMSO-*d*₆) δ: 7.89 (d, *J* = 8.4 Hz, 2H), 7.53 (d, *J* = 8.4 Hz, 2H), 2.64 (s, 3H), 1.29 (s, 9H); ¹³C NMR (DMSO-*d*₆) δ: 167.6, 159.4, 158.1, 155.1, 154.3, 130.2, 126.6, 126.5, 111.7, 35.1, 31.3, 18.7; MS (*m/z*) 369. The obtained salt **5** (0.8 g, 2.1 mmol) was dissolved in water (15 mL). Then, dimethyl sulfate (0.5 mL, 4 mmol) was added dropwise with vigorous stirring. After 2 h, the formed solid was filtered and washed with copious amounts of water to yield the titled compound **6** as a yellowish white solid (0.68 g, 91%); mp = 173 °C; ¹H NMR (DMSO-*d*₆) δ: 7.93 (d, *J* = 8.4 Hz, 2H), 7.56 (d, *J* = 8.4 Hz, 2H), 2.77 (s, 3H), 2.68 (s, 3H), 1.31 (s, 9H); ¹³C NMR (DMSO-*d*₆) δ: 166.5, 162.5, 159.4, 153.9, 153.4, 130.5, 126.5, 126.4, 106.5, 39.3, 35.1, 28.2, 18.6; MS (*m/z*) 345; anal. calc. for: (C₁₇H₁₉N₃OS₂): C, 59.10; H, 5.54; N, 12.16%; found: C, 59.12; H, 5.55; N, 12.17%.

4.1.4. 2-(2-(4-(*tert*-Butyl)phenyl)-4-methylthiazol-5-yl)-5-(methylsulfonyl)-1,3,4-oxadiazole (7). To a solution of **6** (0.5 g, 1.3 mmol) in dry DCM (5 mL), *m*-CPBA (0.514 g, 2.9 mmol) diluted with DCM (5 mL) was added portion-wise with continuous stirring. Afterward, the reaction mixture was kept at 23 °C for 16 h, additional DCM (10 mL) was added and the reaction mixture was washed with 25 mL of 5% aqueous solution of sodium metabisulfite, and 25 mL of 5% aqueous sodium carbonate. The organic layer was separated, dried and concentrated under reduced pressure to give the desired product as yellow crystals (0.5 g, 93%) mp = 144 °C; ¹H NMR (DMSO-*d*₆) δ: 7.88 (d, *J* = 8.4 Hz, 2H), 7.50 (d, *J* = 8.4 Hz, 2H), 3.47 (s, 3H), 2.76 (s, 3H), 1.29 (s, 9H); ¹³C NMR (DMSO-*d*₆) δ: 165.3, 159.2, 159.0, 158.3, 157.0, 130.1, 126.7, 126.6, 118.4, 42.2, 35.1, 31.2, 18.9; MS (*m/z*) 377; anal. calc. for: (C₁₇H₁₉N₃O₃S₂): C, 54.09; H, 5.07; N, 11.13%; found: C, 54.11; H, 5.08; N, 11.15%.

4.2. Compounds 8–30

4.2.1. General procedure. To a solution of **7** (0.1 g, 0.25 mmol) in dry DMF (5 mL), appropriate amine, hydrazine, guanidine or carboximide (0.4 mmol); namely: methylamine, ethylamine, butylamine, isopropylamine, cyclopentylamine, cyclohexylamine, dimethylamine, azetidine hydrochloride, pyrrolidine, piperidine, morpholine, 4-methylpiperazine, azetidin-3-ol hydrochloride, hydrazine hydrate, guanidine hydrochloride, methylguanidine hydrochloride, 1,1-



dimethylguanidine hydrochloride, *N,N*-tetramethyl guanidine, morpholine-4-carboximidamide hydroiodide, 4-methylpiperazine-1-carboximidamide hydroiodide, picolinimidamide hydrochloride, nicotinimidamide hydrochloride, isonicotinimidamide hydrochloride, was added. The reaction mixture was heated at 80 °C for 0.5–12 h and then poured over ice water (50 mL). The formed solid was extracted with ethyl acetate (10 mL). The organic layer was evaporated under reduced pressure. The obtained crude material was then purified by crystallization or column chromatography. Physical properties and spectral analysis of isolated products are listed below:

4.2.2. 5-(2-(4-(*tert*-Butyl)phenyl)-4-methylthiazol-5-yl)-*N*-methyl-1,3,4-oxadiazol-2-amine (8). Following the general procedure 4.2.1., and using methylamine (13 μ L, 0.4 mmol), compound 8 was obtained as yellow solid (0.08 g, 88%) mp = 223 °C; ^1H NMR (DMSO- d_6) δ : 7.85 (d, J = 8.4 Hz, 2H), 7.77 (brs, 1H), 7.51 (d, J = 8.4 Hz, 2H), 2.87 (s, 3H), 2.61 (s, 3H), 1.30 (s, 9H); ^{13}C NMR (DMSO- d_6) δ : 166.1, 164.2, 154.3, 154.1, 153.8, 130.0, 126.5, 126.5, 115.0, 35.1, 29.5, 26.8, 17.3; MS (m/z) 328; HRMS (EI) m/z 328.1358 M^+ , calcd for $\text{C}_{17}\text{H}_{20}\text{N}_4\text{OS}$ 328.1358; anal. calc. for: ($\text{C}_{17}\text{H}_{20}\text{N}_4\text{OS}$): C, 62.17; H, 6.14; N, 17.06%; found: C, 62.18; H, 6.15; N, 17.07%.

4.2.3. 5-(2-(4-(*tert*-Butyl)phenyl)-4-methylthiazol-5-yl)-*N*-ethyl-1,3,4-oxadiazol-2-amine (9). Following the general procedure 4.2.1., and using ethylamine (18 μ L, 0.4 mmol), compound 9 was obtained as yellow solid (0.05 g, 55%) mp = 200 °C; ^1H NMR (DMSO- d_6) δ : 8.26 (brs, 1H), 7.90 (d, J = 8.4 Hz, 2H), 7.54 (d, J = 8.4 Hz, 2H), 3.21 (m, 2H), 2.68 (s, 3H), 1.37 (s, 9H), 1.14 (m, 3H); ^{13}C NMR (DMSO- d_6) δ : 166.0, 163.5, 154.3, 154.1, 153.7, 130.0, 126.8, 126.6, 115.0, 37.9, 34.6, 31.3, 17.4, 15.17; MS (m/z) 342; HRMS (EI) m/z 342.1514 M^+ , calcd for $\text{C}_{18}\text{H}_{22}\text{N}_4\text{OS}$ 342.1514; anal. calc. for: ($\text{C}_{18}\text{H}_{22}\text{N}_4\text{OS}$): C, 63.13; H, 6.48; N, 16.36%; found: C, 63.15; H, 6.50; N, 16.37%.

4.2.4. *N*-Butyl-5-(2-(4-(*tert*-butyl)phenyl)-4-methylthiazol-5-yl)-1,3,4-oxadiazol-2-amine (10). Following the general procedure 4.2.1., and using ethylamine (29 μ L, 0.4 mmol), compound 10 was obtained as yellow solid (0.09 g, 93%) mp = 145 °C; ^1H NMR (DMSO- d_6) δ : 7.88 (d, J = 8.4 Hz, 2H), 7.83 (brs, 1H), 7.53 (d, J = 8.4 Hz, 2H), 3.37 (t, J = 3.2 Hz, 2H), 2.66 (s, 3H), 1.94 (m, 2H), 1.70 (m, 2H), 1.54 (m, 3H), 1.29 (s, 9H); ^{13}C NMR (DMSO- d_6) δ : 166.4, 162.9, 154.3, 153.7, 152.7, 130.0, 126.6, 126.5, 128.6, 127.9, 127.3, 127.1, 115.4, 42.7, 31.2, 19.8, 17.4, 14.0; MS (m/z) 370; HRMS (EI) m/z 370.1827 M^+ , calcd for $\text{C}_{20}\text{H}_{26}\text{N}_4\text{OS}$ 370.1827; anal. calc. for: ($\text{C}_{20}\text{H}_{26}\text{N}_4\text{OS}$): C, 64.83; H, 7.07; N, 15.12%; found: C, 64.84; H, 7.09; N, 15.13%.

4.2.5. 5-(2-(4-(*tert*-Butyl)phenyl)-4-methylthiazol-5-yl)-*N*-isopropyl-1,3,4-oxadiazol-2-amine (11). Following the general procedure 4.2.1., and using ethylamine (23 μ L, 0.4 mmol), compound 11 was obtained as yellow solid (0.06 g, 81%) mp = 220 °C; ^1H NMR (DMSO- d_6) δ : 7.88 (d, J = 8.4 Hz, 2H), 7.82 (brs, 1H), 7.53 (d, J = 8.4 Hz, 2H), 3.70 (m, 1H), 2.65 (s, 3H), 1.29 (s, 9H), 1.20 (d, J = 6.8 Hz, 6H); ^{13}C NMR (DMSO- d_6) δ : 166.5, 162.9, 154.3, 153.7, 152.8, 130.0, 126.6, 126.6, 115.0, 45.4, 35.1, 31.3, 22.7, 17.3; MS (m/z) 356; HRMS (EI) m/z 356.1671 M^+ , calcd for $\text{C}_{19}\text{H}_{24}\text{N}_4\text{OS}$ 356.1671; anal. calc. for: ($\text{C}_{19}\text{H}_{24}\text{N}_4\text{OS}$): C, 64.02; H, 6.79; N, 15.72%; found: C, 64.02; H, 6.80; N, 15.73%.

4.2.6. 5-(2-(4-(*tert*-Butyl)phenyl)-4-methylthiazol-5-yl)-*N*-cyclopentyl-1,3,4-oxadiazol-2-amine (12). Following the general procedure 4.2.1., and using cyclopentylamine (34 μ L, 0.4 mmol), compound 12 was obtained as yellow solid (0.06 g, 60%) mp = 195 °C; ^1H NMR (DMSO- d_6) δ : 7.95 (brs, 1H), 7.86 (d, J = 8.4 Hz, 2H), 7.51 (d, J = 8.4 Hz, 2H), 3.87 (m, 1H), 2.65 (s, 3H), 1.91 (m, 2H), 1.65 (m, 2H), 1.58 (m, 4H), 1.28 (s, 9H); ^{13}C NMR (DMSO- d_6) δ : 166.4, 163.2, 154.3, 153.7, 152.8, 130.0, 126.6, 126.5, 115.0, 54.8, 35.1, 32.6, 31.2, 23.6, 17.3; MS (m/z) 382; HRMS (EI) m/z 382.1827 M^+ , calcd for $\text{C}_{21}\text{H}_{26}\text{N}_4\text{OS}$ 382.1827; anal. calc. for: ($\text{C}_{21}\text{H}_{26}\text{N}_4\text{OS}$): C, 65.94; H, 6.85; N, 14.65%; found: C, 65.96; H, 6.86; N, 14.67%.

4.2.7. 5-(2-(4-(*tert*-Butyl)phenyl)-4-methylthiazol-5-yl)-*N*-cyclohexyl-1,3,4-oxadiazol-2-amine (13). Following the general procedure 4.2.1., and using cyclohexylamine (39 μ L, 0.4 mmol), compound 13 was obtained as light brown solid (0.08 g, 76%) mp = 186 °C; ^1H NMR (DMSO- d_6) δ : 7.95 (brs, 1H), 7.88 (d, J = 8.4 Hz, 2H), 7.53 (d, J = 8.4 Hz, 2H), 3.22 (m, 1H), 2.65 (s, 3H), 1.54 (m, 4H), 1.32 (m, 4H), 1.29 (s, 2H), 0.90 (m, 2H); ^{13}C NMR (DMSO- d_6) δ : 166.5, 163.6, 154.3, 153.7, 152.8, 130.0, 126.6, 126.5, 115.0, 42.7, 35.1, 31.3, 31.2, 19.8, 17.3, 14.0; MS (m/z) 396; HRMS (EI) m/z 396.1984 M^+ , calcd for $\text{C}_{22}\text{H}_{28}\text{N}_4\text{OS}$ 396.1984; anal. calc. for: ($\text{C}_{22}\text{H}_{28}\text{N}_4\text{OS}$): C, 66.63; H, 7.12; N, 14.13%; found: C, 66.64; H, 7.13; N, 14.14%.

4.2.8. 5-(2-(4-(*tert*-Butyl)phenyl)-4-methylthiazol-5-yl)-*N,N*-dimethyl-1,3,4-oxadiazol-2-amine (14). Following the general procedure 4.2.1., and using dimethylamine (18 μ L, 0.4 mmol), compound 14 was obtained as yellow solid (0.07 g, 80%) mp = 185 °C; ^1H NMR (DMSO- d_6) δ : 7.89 (d, J = 8.4 Hz, 2H), 7.53 (d, J = 8.4 Hz, 2H), 3.04 (s, 6H), 2.66 (s, 3H), 1.29 (s, 9H); ^{13}C NMR (DMSO- d_6) δ : 166.6, 164.6, 154.4, 153.9, 153.5, 130.0, 126.6, 126.6, 114.9, 38.1, 35.1, 31.3, 17.3; MS (m/z) 342; HRMS (EI) m/z 342.1514 M^+ , calcd for $\text{C}_{18}\text{H}_{22}\text{N}_4\text{OS}$ 342.1514; anal. calc. for: ($\text{C}_{18}\text{H}_{22}\text{N}_4\text{OS}$): C, 63.13; H, 6.48; N, 16.36%; found: C, 63.14; H, 6.50; N, 16.37%.

4.2.9. 2-(Azetidin-1-yl)-5-(2-(4-(*tert*-butyl)phenyl)-4-methylthiazol-5-yl)-1,3,4-oxadiazole (15). Following the general procedure 4.2.1., and using azetidine hydrochloride (0.04 g, 0.4 mmol), compound 15 was obtained as yellow solid (0.07 g, 70%) mp = 228 °C; ^1H NMR (DMSO- d_6) δ : 7.89 (d, J = 8.4 Hz, 2H), 7.52 (d, J = 8.4 Hz, 2H), 4.14 (t, J = 8 Hz, 4H), 2.87 (m, 2H), 2.69 (s, 3H), 1.28 (s, 9H); ^{13}C NMR (DMSO- d_6) δ : 166.9, 164.7, 162.7, 154.4, 154.3, 129.9, 126.6, 126.5, 114.6, 52.5, 35.1, 31.2, 17.8, 17.3; MS (m/z) 354; HRMS (EI) m/z 354.1514 M^+ , calcd for $\text{C}_{19}\text{H}_{22}\text{N}_4\text{OS}$ 354.1514; anal. calc. for: ($\text{C}_{19}\text{H}_{22}\text{N}_4\text{OS}$): C, 64.38; H, 6.26; N, 15.81%; found: C, 64.40; H, 6.27; N, 15.83%.

4.2.10. 2-(2-(4-(*tert*-Butyl)phenyl)-4-methylthiazol-5-yl)-5-(pyrrolidin-1-yl)-1,3,4-oxadiazole (16). Following the general procedure 4.2.1., and using pyrrolidine (28 μ L, 0.4 mmol), compound 16 was obtained as yellow solid (0.089 g, 91%) mp = 226 °C; ^1H NMR (DMSO- d_6) δ : 7.89 (d, J = 8.4 Hz, 2H), 7.53 (d, J = 8.4 Hz, 2H), 3.48 (m, 4H), 2.65 (s, 3H), 1.96 (m, 4H), 1.27 (s, 9H); ^{13}C NMR (DMSO- d_6) δ : 166.5, 162.4, 154.4, 153.8, 153.2, 130.0, 126.63, 126.61, 114.2, 48.0, 35.1, 31.3, 25.5, 17.3; MS (m/z) 368; HRMS (EI) m/z 368.1671 M^+ , calcd for $\text{C}_{20}\text{H}_{24}\text{N}_4\text{OS}$ 368.1671; anal. calc. for: ($\text{C}_{20}\text{H}_{24}\text{N}_4\text{OS}$): C, 65.19; H, 6.57; N, 15.20%; found: C, 65.20; H, 6.58; N, 15.21%.



4.2.11. 2-(2-(4-(*tert*-Butyl)phenyl)-4-methylthiazol-5-yl)-5-(piperidin-1-yl)-1,3,4-oxadiazole (17). Following the general procedure 4.2.1., and using piperidine (34 μ L, 0.4 mmol), compound 17 was obtained as yellow solid (0.098 g, 97%) mp = 285 °C; ^1H NMR (DMSO- d_6) δ : 7.89 (d, J = 8.4 Hz, 2H), 7.54 (d, J = 8.4 Hz, 2H), 3.45 (m, 4H), 2.66 (s, 3H), 1.59 (m, 6H), 1.29 (s, 9H); ^{13}C NMR (DMSO- d_6) δ : 166.7, 164.0, 154.4, 154.0, 153.5, 130.0, 126.64, 126.63, 114.8, 47.1, 35.1, 31.3, 24.8, 23.6, 17.4; MS (m/z) 382; HRMS (EI) m/z 382.1827 M^+ , calcd for $\text{C}_{21}\text{H}_{26}\text{N}_4\text{OS}$ 382.1827; anal. calc. for: ($\text{C}_{21}\text{H}_{26}\text{N}_4\text{OS}$): C, 65.94; H, 6.85; N, 14.65%; found: C, 65.95; H, 6.87; N, 14.67%.

4.2.12. 4-(5-(2-(4-(*tert*-Butyl)phenyl)-4-methylthiazol-5-yl)-1,3,4-oxadiazol-2-yl)morpholine (18). Following the general procedure 4.2.1., and using morpholine (35 μ L, 0.4 mmol), compound 18 was obtained as yellow solid (0.098 g, 97%) mp = 285 °C; ^1H NMR (DMSO- d_6) δ : 7.99 (d, J = 8.4 Hz, 2H), 7.57 (d, J = 8.4 Hz, 2H), 3.73 (m, 4H), 3.48 (m, 4H), 2.68 (s, 3H), 1.32 (s, 9H); ^{13}C NMR (DMSO- d_6) δ : 167.0, 164.0, 154.5, 154.0, 153.1, 130.0, 126.6, 126.3, 114.7, 65.6, 46.2, 35.2, 31.3, 17.4; MS (m/z) 384; HRMS (EI) m/z 384.1620 M^+ , calcd for $\text{C}_{20}\text{H}_{24}\text{N}_4\text{O}_2\text{S}$ 384.1620; anal. calc. for: ($\text{C}_{20}\text{H}_{24}\text{N}_4\text{O}_2\text{S}$): C, 62.48; H, 6.29; N, 14.57%; found: C, 62.49; H, 6.30; N, 14.59%.

4.2.13. 2-(2-(4-(*tert*-Butyl)phenyl)-4-methylthiazol-5-yl)-5-(4-methylpiperazin-1-yl)-1,3,4-oxadiazole (19). Following the general procedure 4.2.1., and using 4-methylpiperazine (40 μ L, 0.4 mmol), compound 19 was obtained as yellow solid (0.099 g, 97%) mp = 177 °C; ^1H NMR (DMSO- d_6) δ : 7.84 (d, J = 8.4 Hz, 2H), 7.52 (d, J = 8.4 Hz, 2H), 3.47 (m, 4H), 2.66 (s, 3H), 2.25 (m, 4H), 2.14 (s, 3H), 1.28 (s, 9H); ^{13}C NMR (DMSO- d_6) δ : 166.8, 163.8, 161.8, 157.1, 156.4, 130.2, 126.6, 126.5, 114.7, 53.7, 46.0, 43.8, 35.1, 31.3, 17.5; MS (m/z) 397; HRMS (EI) m/z 397.1936 M^+ , calcd for $\text{C}_{21}\text{H}_{27}\text{N}_5\text{OS}$ 397.1936; anal. calc. for: ($\text{C}_{21}\text{H}_{27}\text{N}_5\text{OS}$): C, 63.45; H, 6.85; N, 17.62%; found: C, 63.47; H, 6.87; N, 17.64%.

4.2.14. 1-(5-(2-(4-(*tert*-Butyl)phenyl)-4-methylthiazol-5-yl)-1,3,4-oxadiazol-2-yl)azetidin-3-ol (20). Following the general procedure 4.2.1., and using azetidin-3-ol hydrochloride (0.04 g, 0.4 mmol), compound 20 was obtained as yellow solid (0.05 g, 54%) mp = 210 °C; ^1H NMR (DMSO- d_6) δ : 7.88 (d, J = 8.4 Hz, 2H), 7.52 (d, J = 8.4 Hz, 2H), 6.06 (brs, 1H), 4.66 (m, 1H), 4.35 (dd, J = 7.6 Hz, J = 8.4 Hz, 2H), 3.97 (dd, J = 5.2 Hz, J = 8.2 Hz, 2H), 2.65 (s, 3H), 1.29 (s, 9H); ^{13}C NMR (DMSO- d_6) δ : 166.9, 164.7, 154.49, 154.45, 154.42, 129.9, 126.6, 126.4, 114.6, 62.3, 62.1, 35.1, 31.3, 17.4; MS (m/z) 370; HRMS (EI) m/z 370.1463 M^+ , calcd for $\text{C}_{19}\text{H}_{22}\text{N}_4\text{O}_2\text{S}$ 370.1463; anal. calc. for: ($\text{C}_{19}\text{H}_{22}\text{N}_4\text{O}_2\text{S}$): C, 61.60; H, 5.99; N, 15.12%; found: C, 61.61; H, 6.01; N, 15.13%.

4.2.15. 2-(2-(4-(*tert*-Butyl)phenyl)-4-methylthiazol-5-yl)-5-hydrazinyl-1,3,4-oxadiazole (21). Following the general procedure 4.2.1., and using hydrazine hydrate (5 mL), compound 21 was obtained as yellow fluffy powder (0.06 g, 75%) mp = 260 °C; ^1H NMR (DMSO- d_6) δ : 7.85 (d, J = 8.4 Hz, 2H), 7.50 (d, J = 8.4 Hz, 2H), 6.94 (brs, 1H), 4.54 (brs, 2H), 2.62 (s, 3H), 1.31 (s, 9H); ^{13}C NMR (DMSO- d_6) δ : 166.3, 163.2, 155.7, 155.2, 154.1, 130.3, 126.6, 126.5, 124.6, 35.1, 31.3, 17.5; MS (m/z) 329; HRMS (EI) m/z 329.1310 M^+ , calcd for $\text{C}_{16}\text{H}_{19}\text{N}_5\text{OS}$ 329.1310; anal. calc. for: ($\text{C}_{16}\text{H}_{19}\text{N}_5\text{OS}$): C, 58.34; H, 5.81; N, 21.26%; found: C, 58.36; H, 5.82; N, 21.26%.

4.2.16. 1-(5-(2-(4-(*tert*-Butyl)phenyl)-4-methylthiazol-5-yl)-1,3,4-oxadiazol-2-yl)guanidine (22). Following the general procedure 4.2.1., and using guanidine hydrochloride (0.05 g, 0.5 mmol), compound 22 was obtained as grayish solid (0.07 g, 76%) mp = 198 °C; ^1H NMR (DMSO- d_6) δ : 7.88 (d, J = 8.4 Hz, 2H), 7.53 (d, J = 8.4 Hz, 2H), 7.21 (brs, 1H), 7.06 (brs, 3H), 2.65 (s, 3H), 1.29 (s, 9H); ^{13}C NMR (DMSO- d_6) δ : 167.2, 166.5, 159.5, 154.3, 153.7, 152.6, 130.0, 126.6, 126.5, 115.7, 35.1, 31.3, 17.3; MS (m/z) 356; HRMS (EI) m/z 356.1419 M^+ , calcd for $\text{C}_{17}\text{H}_{20}\text{N}_6\text{OS}$ 356.1419; anal. calc. for: ($\text{C}_{17}\text{H}_{20}\text{N}_6\text{OS}$): C, 57.28; H, 5.66; N, 23.58%; found: C, 57.30; H, 5.67; N, 23.60%.

4.2.17. 1-(5-(2-(4-(*tert*-Butyl)phenyl)-4-methylthiazol-5-yl)-1,3,4-oxadiazol-2-yl)-3-methylguanidine (23). Following the general procedure 4.2.1., and using methylguanidine hydrochloride (0.06 g, 0.5 mmol), compound 23 was obtained as yellowish brown solid (0.07 g, 75%) mp = 194 °C; ^1H NMR (DMSO- d_6) δ : 7.89 (d, J = 8.4 Hz, 2H), 7.81 (brs, 1H), 7.54 (d, J = 8 Hz, 2H), 7.37 (brs, 1H), 2.87 (s, 3H), 2.78 (brs, 1H), 2.67 (s, 3H), 1.30 (s, 9H); ^{13}C NMR (DMSO- d_6) δ : 166.5, 164.2, 154.3, 153.8, 153.0, 130.1, 130.0, 126.6, 126.5, 115.0, 35.1, 31.3, 29.5, 17.4; MS (m/z) 370; HRMS (EI) m/z 370.1576 M^+ , calcd for $\text{C}_{18}\text{H}_{22}\text{N}_6\text{OS}$ 370.1576; anal. calc. for: ($\text{C}_{18}\text{H}_{22}\text{N}_6\text{OS}$): C, 58.36; H, 5.99; N, 22.68%; found: C, 58.37; H, 5.99; N, 22.69%.

4.2.18. 3-(5-(2-(4-(*tert*-Butyl)phenyl)-4-methylthiazol-5-yl)-1,3,4-oxadiazol-2-yl)-1,1-dimethylguanidine (24). Following the general procedure 4.2.1., and using 1,1-dimethylguanidine hydrochloride (0.06 g, 0.5 mmol), compound 24 was obtained as yellowish brown solid (0.08 g, 75%) mp = 194 °C; ^1H NMR (DMSO- d_6) δ : 7.89 (d, J = 8.4 Hz, 2H), 7.75 (brs, 2H), 7.54 (d, J = 8 Hz, 2H), 3.01 (s, 6H), 2.68 (s, 3H), 1.29 (s, 9H); ^{13}C NMR (DMSO- d_6) δ : 166.8, 166.6, 157.8, 154.3, 153.9, 152.8, 130.1, 126.63, 126.60, 115.7, 37.5, 35.1, 31.3, 17.5; MS (m/z) 384; HRMS (EI) m/z 384.1732 M^+ , calcd for $\text{C}_{19}\text{H}_{24}\text{N}_6\text{OS}$ 384.1732; anal. calc. for: ($\text{C}_{19}\text{H}_{24}\text{N}_6\text{OS}$): C, 59.35; H, 6.29; N, 21.86%; found: C, 59.35; H, 6.29; N, 21.86%.

4.2.19. 2-(5-(2-(4-(*tert*-Butyl)phenyl)-4-methylthiazol-5-yl)-1,3,4-oxadiazol-2-yl)-1,1,3,3-tetramethylguanidine (25). Following the general procedure 4.2.1., and using *N,N*-tetramethyl guanidine (50 μ L, 0.4 mmol), compound 25 was obtained as yellowish brown solid (0.08 g, 75%) mp = 194 °C; ^1H NMR (DMSO- d_6) δ : 7.88 (d, J = 8.4 Hz, 2H), 7.52 (d, J = 8.4 Hz, 2H), 2.81 (s, 12H), 2.66 (s, 3H), 1.28 (s, 9H); ^{13}C NMR (DMSO- d_6) δ : 166.4, 164.9, 163.7, 154.2, 154.1, 153.4, 130.1, 126.6, 126.5, 115.8, 139.3, 35.1, 31.3, 17.4; MS (m/z) 412; HRMS (EI) m/z 412.2045 M^+ , calcd for $\text{C}_{21}\text{H}_{28}\text{N}_6\text{OS}$ 412.2045; anal. calc. for: ($\text{C}_{21}\text{H}_{28}\text{N}_6\text{OS}$): C, 61.14; H, 6.84; N, 20.37%; found: C, 61.15; H, 6.86; N, 20.38%.

4.2.20. *N*-(5-(2-(4-(*tert*-Butyl)phenyl)-4-methylthiazol-5-yl)-1,3,4-oxadiazol-2-yl)morpholine-4-carboximidamide (26). Following the general procedure 4.2.1., and using morpholine-4-carboximidamide hydroiodide (0.1 g, 0.4 mmol), compound 26 was obtained as yellow solid (0.07 g, 65%) mp = 260 °C; ^1H NMR (DMSO- d_6) δ : 7.96 (brs, 2H), 7.90 (d, J = 8.4 Hz, 2H), 7.54 (d, J = 8.4 Hz, 2H), 3.64 (m, 4H), 3.56 (m, 4H), 2.69 (s, 3H), 1.31 (s, 9H); ^{13}C NMR (DMSO- d_6) δ : 166.9, 166.8, 157.2, 154.3, 154.1, 153.2, 130.0, 126.6, 126.5, 115.4, 66.1, 44.8, 35.1, 31.3, 17.5; MS



(*m/z*) 426; HRMS (EI) *m/z* 426.1838 M⁺, calcd for C₂₁H₂₆N₆O₂S 426.1838; anal. calc. for: (C₂₁H₂₆N₆O₂S): C, 59.13; H, 6.14; N, 19.70%; found: C, 59.15; H, 6.15; N, 19.72%.

4.2.21. *N*-(5-(2-(4-(*tert*-Butyl)phenyl)-4-methylthiazol-5-yl)-1,3,4-oxadiazol-2-yl)-4-methylpiperazine-1-carboximidamide (27). Following the general procedure 4.2.1., and using 4-methylpiperazine-1-carboximidamide hydroiodide (0.11 g, 0.4 mmol), compound 27 was obtained as yellow solid (0.07 g, 63%) mp = 262 °C; ¹H NMR (DMSO-*d*₆) δ: 7.98 (brs, 2H), 7.92 (d, *J* = 8.4 Hz, 2H), 7.52 (d, *J* = 8.4 Hz, 2H), 3.58 (m, 4H), 2.68 (s, 3H), 2.35 (m, 4H), 2.21 (s, 3H), 1.30 (s, 9H); ¹³C NMR (DMSO-*d*₆) δ: 166.9, 166.6, 156.9, 154.3, 154.0, 153.0, 130.0, 126.59, 126.56, 115.5, 54.5, 45.9, 44.3, 35.1, 31.3, 17.5; MS (*m/z*) 439; HRMS (EI) *m/z* 439.2154 M⁺, calcd for C₂₂H₂₉N₇OS 439.2154; anal. calc. for: (C₂₂H₂₉N₇OS): C, 60.11; H, 6.65; N, 22.31%; found: C, 60.12; H, 6.67; N, 22.33%.

4.2.22. *N*-(5-(2-(4-(*tert*-Butyl)phenyl)-4-methylthiazol-5-yl)-1,3,4-oxadiazol-2-yl)picolinimidamide (28). Following the general procedure 4.2.1., and using picolinimidamide hydrochloride (0.06 g, 0.4 mmol), compound 28 was obtained as yellow solid (0.1 g, 91%) mp = 225 °C; ¹H NMR (DMSO-*d*₆) δ: 9.43 (brs, 1H), 8.92 (brs, 1H), 8.76 (m, 1H), 8.34 (m, 1H), 7.94–7.82 (m, 3H), 7.57–7.49 (m, 3H), 2.68 (s, 3H), 1.30 (s, 9H); ¹³C NMR (DMSO-*d*₆) δ: 167.2, 166.9, 162.8, 158.4, 158.0, 154.2, 153.9, 149.0, 138.0, 131.7, 130.5, 126.5, 126.4, 122.6, 111.4, 35.1, 31.3, 18.7; MS (*m/z*) 418; HRMS (EI) *m/z* 418.1576 M⁺, calcd for C₂₂H₂₂N₆OS 418.1576; anal. calc. for: (C₂₂H₂₂N₆OS): C, 63.14; H, 5.30; N, 20.08%; found: C, 63.15; H, 5.31; N, 20.09%.

4.2.23. *N*-(5-(2-(4-(*tert*-Butyl)phenyl)-4-methylthiazol-5-yl)-1,3,4-oxadiazol-2-yl)nicotinimidamide (29). Following the general procedure 4.2.1., and using nicotinimidamide hydrochloride (0.06 g, 0.4 mmol), compound 29 was obtained as yellow solid (0.1 g, 91%) mp = 289 °C; ¹H NMR (DMSO-*d*₆) δ: 9.78 (brs, 1H), 9.24 (s, 1H), 9.02 (brs, 1H), 8.75 (d, *J* = 6.8 Hz, 1H), 8.46 (t, *J* = 6.6 Hz, 1H), 7.95 (d, *J* = 8.4 Hz, 2H), 7.56 (m, 3H), 2.71 (s, 3H), 1.28 (s, 9H); ¹³C NMR (DMSO-*d*₆) δ: 167.6, 166.4, 160.5, 155.4, 155.1, 154.5, 152.8, 149.2, 135.9, 130.6, 129.6, 126.5, 126.4, 123.9, 114.8, 35.1, 31.3, 17.6; MS (*m/z*) 418; HRMS (EI) *m/z* 418.1576 M⁺, calcd for C₂₂H₂₂N₆OS 418.1576; anal. calc. for: (C₂₂H₂₂N₆OS): C, 63.14; H, 5.30; N, 20.08%; found: C, 63.16; H, 5.32; N, 20.10%.

4.2.24. *N*-(5-(2-(4-(*tert*-Butyl)phenyl)-4-methylthiazol-5-yl)-1,3,4-oxadiazol-2-yl)isonicotinimidamide (30). Following the general procedure 4.2.1., and using isonicotinimidamide hydrochloride (0.06 g, 0.4 mmol), compound 30 was obtained as yellow solid (0.07 g, 64%) mp = 257 °C; ¹H NMR (DMSO-*d*₆) δ: 9.83 (brs, 1H), 9.05 (brs, 1H), 8.77 (d, *J* = 7.6 Hz, 2H), 7.89 (d, *J* = 7.6 Hz, 2H), 7.83 (d, *J* = 8.4 Hz, 2H), 7.52 (d, *J* = 8.4 Hz, 2H), 2.73 (s, 3H), 1.29 (s, 9H); ¹³C NMR (DMSO-*d*₆) δ: 167.7, 166.3, 160.2, 155.5, 154.5, 153.9, 150.7, 141.1, 130.0, 126.6, 126.4, 121.9, 114.7, 35.1, 31.2, 17.6; MS (*m/z*) 418; HRMS (EI) *m/z* 418.1576 M⁺, calcd for C₂₂H₂₂N₆OS 418.1576; anal. calc. for: (C₂₂H₂₂N₆OS): C, 63.14; H, 5.30; N, 20.08%; found: C, 63.16; H, 5.31; N, 20.09%.

4.3. Microbiological assays

4.3.1. Determination of minimum inhibitory concentration (MIC) and minimum bactericidal concentration (MBC).

Broth microdilution method was used^{18,19} against a panel of clinically important Gram positive bacterial pathogens according to the previous reports.^{19,20}

4.3.2. Time-kill assay against MRSA. It was performed against MRSA USA400 as described previously.^{20,21} In brief, bacterial cells in logarithmic phase were diluted and drugs were added at 5× MIC and 10× MIC (in triplicates). After time points, cells were collected, diluted and plated on tryptic soy agar plates. Plates were incubated for 18–20 hours and the viable CFU mL^{−1} was determined.

4.3.3. MRSA biofilm eradication assessment. Compound 20 was examined for its ability to eradicate established, mature staphylococcal biofilm using the microtiter plate biofilm formation assay following the procedure described before.^{7,22,23}

4.3.4. *In vivo* pharmacokinetics. Pharmacokinetic studies were performed following the procedure described in a previous report.⁵

Conflicts of interest

There are no conflicts to declare.

Acknowledgements

This work was funded by Science & Technology Development Funds (STDF-Egypt) and the Egyptian Ministry of Higher Education and Scientific Research (MHESR). The work is derived from the Subject Data funded in whole or part by NAS and USAID, and that any opinions, findings, conclusions, or recommendations expressed in such article are those of the authors alone, and do not necessarily reflect the views of USAID or NAS. The authors would like to thank BEI Resources for providing clinical isolates of *S. aureus* used in this study.

Notes and references

- 1 M. Hagrass, Y. A. Hegazy, A. H. Elkabbany, H. Mohammad, A. Ghiaty, T. M. Abdelghany, M. N. Seleem and A. S. Mayhoub, *Eur. J. Med. Chem.*, 2018, **143**, 1448–1456.
- 2 H. Mohammad, A. S. Mayhoub, A. Ghafoor, M. Soofi, R. A. Alajlouni, M. Cushman and M. N. Seleem, *J. Med. Chem.*, 2014, **57**, 1609–1615.
- 3 H. Mohammad, W. Younis, L. Chen, C. E. Peters, J. Pogliano, K. Pogliano, B. Cooper, J. Zhang, A. Mayhoub, E. Oldfield, M. Cushman and M. N. Seleem, *J. Med. Chem.*, 2017, **60**, 2425–2438.
- 4 M. Hagrass, H. Mohammad, M. S. Mandour, Y. A. Hegazy, A. Ghiaty, M. N. Seleem and A. S. Mayhoub, *J. Med. Chem.*, 2017, **60**, 4074–4085.
- 5 M. A. Seleem, A. M. Disouky, H. Mohammad, T. M. Abdelghany, A. S. Mancy, S. A. Bayoumi, A. Elshafeey, A. El-Morsy, M. N. Seleem and A. S. Mayhoub, *J. Med. Chem.*, 2016, **59**, 4900–4912.
- 6 E. Yahia, H. Mohammad, T. M. Abdelghany, E. Fayed, M. N. Seleem and A. S. Mayhoub, *Eur. J. Med. Chem.*, 2017, **126**, 604–613.



- 7 A. Kotb, N. S. Abutaleb, M. A. Seleem, M. Hagra, H. Mohammad, A. Bayoumi, A. Ghiaty, M. N. Seleem and A. S. Mayhoub, *Eur. J. Med. Chem.*, 2018, **151**, 110–120.
- 8 I. Eid, M. M. Elsebaei, H. Mohammad, M. Hagra, C. E. Peters, Y. A. Hegazy, B. Cooper, J. Pogliano, K. Pogliano, H. S. Abulkhair, M. N. Seleem and A. S. Mayhoub, *Eur. J. Med. Chem.*, 2017, **139**, 665–673.
- 9 H. Mohammad, A. AbdelKhalek, N. S. Abutaleb and M. N. Seleem, *Int. J. Antimicrob. Agents*, 2018, **51**, 897–904.
- 10 A. AbdelKhalek, N. S. Abutaleb, K. A. Elmagarmid and M. N. Seleem, *Sci. Rep.*, 2018, **8**, 8353.
- 11 A. AbdelKhalek, N. S. Abutaleb, H. Mohammad and M. N. Seleem, *PLoS One*, 2018, **13**, e0199710.
- 12 R. J. McLean, J. S. Lam and L. L. Graham, *J. Bacteriol.*, 2012, **194**, 6706–6711.
- 13 R. Cavaliere, J. L. Ball, L. Turnbull and C. B. Whitchurch, *MicrobiologyOpen*, 2014, **3**, 557–567.
- 14 R. Wang, B. A. Khan, G. Y. Cheung, T. H. Bach, M. Jameson-Lee, K. F. Kong, S. Y. Queck and M. Otto, *J. Clin. Invest.*, 2011, **121**, 238–248.
- 15 D. Davies, *Nat. Rev. Drug Discovery*, 2003, **2**, 114–122.
- 16 L. D. Saravolatz, G. E. Stein and L. B. Johnson, *Clin. Infect. Dis.*, 2011, **52**, 1156–1163.
- 17 C. R. Caulder, A. Sloan, A. Yasir and P. B. Bookstaver, *Hosp. Pharm.*, 2014, **49**, 644–646.
- 18 S. Thangamani, H. Mohammad, M. F. Abushahba, T. J. Sobreira, V. E. Hedrick, L. N. Paul and M. N. Seleem, *Sci. Rep.*, 2016, **6**, 22571.
- 19 H. Mohammad, M. Cushman and M. N. Seleem, *PLoS One*, 2015, **10**, e0130385.
- 20 M. F. Mohamed, M. I. Hamed, A. Panitch and M. N. Seleem, *Antimicrob. Agents Chemother.*, 2014, **58**, 4113–4122.
- 21 M. F. Mohamed, G. K. Hammac, L. Guptill and M. N. Seleem, *PLoS One*, 2014, **9**, e116259.
- 22 G. A. O'Toole, *J. Visualized Exp.*, 2011, **47**, 2437.
- 23 H. Mohammad, A. S. Mayhoub, M. Cushman and M. N. Seleem, *J. Antibiot.*, 2015, **68**, 259–266.

